JOURNAL OF GEOPHYSICAL RESEARCH, VOL. 91, NO. C12, PAGES 14,250–14,260, DECEMBER 15, 1986

Further Development of an Improved Altimeter Wind Speed Algorithm

DUDLEY B. CHELTON

College of Oceanography, Oregon State University, Corvallis

FRANK J. WENTZ

Remote Sensing Systems, Sausalito, California

A previous altimeter wind speed retrieval algorithm was developed on the basis of wind speeds in the limited range from about 4 to 14 ms^{-1}. In this paper, we use a new approach which gives a wind speed model function applicable over the range 0 to 21 ms^{-1}. The method is based on comparing 50 km along-track averages of the altimeter normalized radar cross section measurements with neighboring off-nadir scatterometer wind speed measurements. The scatterometer winds are constructed from 100 km binned measurements of radar cross section and are located approximately 200 km from the satellite subtrack. The new model function agrees very well with earlier versions up to wind speeds of 14 ms^{-1} but differs significantly at higher wind speeds. We discuss the relevance of these results to the Geosat altimeter launched in March 1985.

1. INTRODUCTION

Collection of an adequate in situ data base from which to develop algorithms for retrieval of geophysical parameters is a long-standing problem in satellite remote sensing of the ocean. This is particularly true for the satellite radar altimeter which measures backscattered microwave radiation from only a single circular cell at satellite nadir (the point on the ocean surface directly beneath the satellite). In this paper, we are concerned with altimeter measurements of wind speed which can be inferred from the power of the backscattered signal [*Brown et al.*, 1981; *Fedor and Brown*, 1982; *Chelton and McCabe*, 1985]. The number of measurements "coincident" with in situ data (usually defined to be within 1 hour and 100 km) is far fewer for the altimeter than for satellite sensors such as the scatterometer and passive microwave radiometer which measure the sea surface over many cells across a swath width of 500–1500 km. Thus, development of a reliable wind speed retrieval algorithm by comparison with in situ measurements is considerably more difficult for the altimeter.

Chelton and McCabe [1985], hereafter referred to as CM, recently proposed and implemented a new method for altimeter wind speed algorithm development. The new method assumes the wind speed in ms^{-1} at 19.5 m above the sea surface is related to the normalized radar cross section σ° of the sea surface by the power-law model function

$$\sigma^\circ = \tilde{G} u_{19.5}^{H}$$

Expressing σ° in decibels, this can be written as

$$\sigma^\circ(\text{dB}) = 10[G + H \log_{10} u_{19.5}]$$

This form of the model function is the same as that used for nadir measurements of σ° by the Seasat scatterometer (SASS) [see *Boggs*, 1981; *Schroeder et al.*, 1982]. For the Seasat altimeter (ALT), CM estimated the parameters G and H by least squares from a comparison of global 96-day, 2° latitude by 6° longitude spatial averages of ALT σ° with vertically polarized, off-nadir SASS neutral stability wind speed at 19.5 m. The resulting values were

$$G = 1.502 \qquad H = -0.468$$

In practice, wind speeds are determined from measurements of σ° by inverting this model function to obtain estimated wind speeds $\hat{u}_{19.5}$ by

$$\hat{u}_{19.5} = 10^{[(\sigma^\circ(\text{dB})/10 - G)/H]}$$

As discussed in CM, there were significant errors in the algorithm used by the Seasat Project to compute σ° from the altimeter receiver automatic gain control, satellite attitude angle and satellite height. Alternative algorithms have been proposed by L. Fedor and by D. Hancock. Both of these σ° algorithms were evaluated by CM and found to perform equally well. The Hancock algorithm was chosen to be preferable because of its simpler form.

There are several weaknesses in the wind speed model function proposed by CM. The first is that the SASS data base used for "calibration" of the ALT σ° measurements is known to be flawed. *Wentz et al.* [1984], CM and *Woiceshyn et al.* [1986] have shown that there are a number of systematic errors in the so-called SASS-1 algorithm used by the Seasat Project to retrieve wind speeds. These errors include an overall bias of about 1 m/s in wind speed, an artificial cross-track gradient in winds, a substantial overestimation of low wind speeds, and data gaps for areas of light winds. In addition, the winds computed from horizontally polarized radar observations were inconsistent with those constructed from the vertically polarized observations. However, this polarization error does not affect the CM results because only vertically polarized winds were used in the analysis. The effects of cross-track biases are greatly reduced in the 96-day, 2° by 6° temporal and spatial averages which include individual wind speed estimates over the full SASS incidence angle range from 22° to 55°. However, the 1 ms^{-1} bias is not eliminated in the temporal and spatial averages. Consequently, CM applied a 1 ms^{-1} correction to the SASS data. This ad hoc correction is defensible on the basis of independent estimates by *Wentz et al.* [1984] and CM. In addition, postexperiment calibration in the JASIN experiment revealed that the "standard" wind recorder overestimated wind speeds by about 10%, corresponding to 1

Paper number 6C0488.
0148-0227/86/006C-0488$05.00

ms^{-1} for the 10 ms^{-1} winds typically observed in JASIN [*Weller et al.*, 1983]. The final SASS wind speed algorithm was heavily tuned to the JASIN data, which probably explains the 1 ms^{-1} bias in SASS winds.

A second limitation of the CM ALT wind speed algorithm is that the 96-day, 2° by 6° temporal and spatial averaging resulted in SASS wind speeds limited to the range 4 to 14 ms^{-1}. Wind speeds computed using the CM algorithm agree very well with SASS wind speeds in the temporal and spatial averages over this limited range of winds speeds. However, it is not yet known whether the assumed power-law relationship between σ° and wind speed at satellite nadir is valid outside this range from 4 to 14 ms^{-1}. Indeed, the scatter plot comparison of 96-day, 2° by 6° temporal and spatial averages of ALT and SASS wind speeds (Figure 16 of CM, reproduced here in Figure 6*a* using SASS wind speeds computed by the *Wentz et al.* [1986] algorithm) suggests that ALT estimates may be high for wind speeds above about 12–13 ms^{-1}. There is also a suggestion that ALT estimates are slightly high over the range 4 to 7 ms^{-1}.

Finally, the CM wind speed algorithm is limited by the fact that it is derived only for very long temporal and large spatial averages. It is not yet known how well it performs on individual measurements.

In this paper, we propose a new method for deriving an ALT wind speed model function. This new approach is analogous to that used by *Wentz et al.* [1986] to determine the relationship between the SASS nadir σ° and wind speed. By applying this method to the ALT measurements, the three limitations in the CM algorithm development are eliminated. The technique is based on comparisons between instantaneous ALT measurements of nadir σ° and the nearest off-nadir SASS measurements of wind speed, corresponding to an incidence angle of 24°, or about 200 km separation on the sea surface from satellite nadir. Because of this rather large spatial separation, we do not expect exact agreement between individual nadir ALT and 24° incidence angle SASS wind speeds.

Differences between SASS estimates of wind speed at 24° incidence angle and the actual wind speed at satellite nadir are attributable to (1) errors in the SASS estimate of wind speed, and (2) differences between actual winds at 24° incidence angle and nadir. In view of the previous efforts by *Wentz et al.* [1984, 1986] to remove systematic errors in the SASS winds, we believe the first source of differences to have a mean of zero when averaged globally over the 3-month Seasat mission. The second source of differences will also have a mean of zero when averaged globally over 3 months. Thus, the total differences between off-nadir SASS wind speed estimates and actual winds at nadir will be random with a zero mean. The method is therefore essentially equivalent to comparison of ALT measurements of nadir σ° with in situ measurements of wind speed. To the extent that SASS wind speeds are accurate on the average, the resulting model function for ALT wind speeds will also be accurate on the average.

2. METHOD

As discussed in section 1, the SASS wind speeds generated by the Seasat Project using the SASS-1 wind speed algorithm [see *Boggs*, 1981; *Jones et al.*, 1982] are known to contain a number of systematic errors. These errors are discussed extensively in *Wentz et al.* [1984] and *Woiceshyn et al.* [1986] and SASS winds must be corrected in order to develop an ALT wind speed model function using the method proposed in this paper. *Wentz et al.* [1986] developed a new algorithm for SASS wind speed retrieval which is particularly appealing, in that it is based only on the assumptions that (1) wind speeds over the global ocean are Rayleigh distributed, (2) the average global wind speed is 7.4 ms^{-1}, (3) wind directions over the global ocean measured relative to SASS antenna pointing angle are evenly distributed over all angles from −180° to 180°. The retrieval of wind speed (which is the only wind parameter of interest in this paper) is not sensitive to the validity of the third assumption. The second assumption was rationalized on the basis of July, August and September data in the *U.S. Navy Marine Climatic Atlas* [*Naval Oceanography Command Detachment*, 1981].

One of the most attractive aspects of this SASS wind speed algorithm is that it was derived without the use of any in situ data. The performance of the algorithm can thus be independently tested by comparing the resulting SASS estimates of wind speed with in situ measurements. This comparison has been made by *Wentz et al.* [1986] based on 1623 matches with NDBO buoy measurements within 1 hour and 100 km of the SASS measurements. The rms discrepancy between these two measures of wind speed was 1.6 ms^{-1}, with a small overall bias of −0.1 ms^{-1}. The buoy wind speeds in this comparison ranged from 0 to 17 ms^{-1}. In comparison, when both vertically and horizontally polarized data are included, the SASS-1 algorithm gives a bias of 1.08 ms^{-1} and an rms error about this bias of 2.30 ms^{-1} when compared with the same set of buoy measurements. The better performance of the *Wentz et al.* [1986] algorithm is particularly impressive in view of the fact that it was developed independent of any in situ data.

On the basis of these results, we feel that development of an ALT wind speed model function using SASS wind speeds generated by the *Wentz et al.* [1986] algorithm is far superior to the use of wind speeds generated by the SASS-1 algorithm.

The approximate measurement geometry for ALT and SASS measurements of wind speed is shown in Figure 1. The Seasat altimeter transmitted a nadir-directed short pulse of 13.5 GHz microwave radiation from an antenna with 1.59° beamwidth. For altimeter measurements of sea surface elevation and significant wave height, the pulse length determines the effective footprint size on the sea surface [see *Stewart*, 1985]. However, σ° is determined from the automatic gain control which drives the sum of 63 discrete samples of the return signal to a constant value [*Townsend*, 1980]. Sixty of the sample gates are separated by 3.125 ns with the additional three gates half way between gates 29, 30, 31 and 32. The altitude tracker in the altimeter electronics package centers mean sea level at gate 30.5. Thus, the footprint of the spherically expanding altimeter pulse projected on mean sea level is determined by the area covered over the time interval from gate 30.5 to gate 60 (a total of 92.19 ns). This gate-limited footprint corresponds to a circle with diameter 9.5 km, considerably smaller than the full 22 km footprint corresponding to the 1.59° antenna beamwidth. Thus, the return power measured over the 60 gates is less than the total power returned from the transmitted pulse.

ALT measurements of σ° were averaged over 1 sec (a total of 1020 individual pulses), during which time the 9.5 km circular footprint moves 6.7 km along the satellite ground track. For the purpose of comparing the ALT measurements with the SASS measurements of radar cross section and wind speed, the ALT measurements were averaged over a 50 km segment of the subtrack. This 50 km ALT bin, which consists of about 7 ALT footprints, is shown in Figure 1.

The Seasat SASS used a different method for measuring

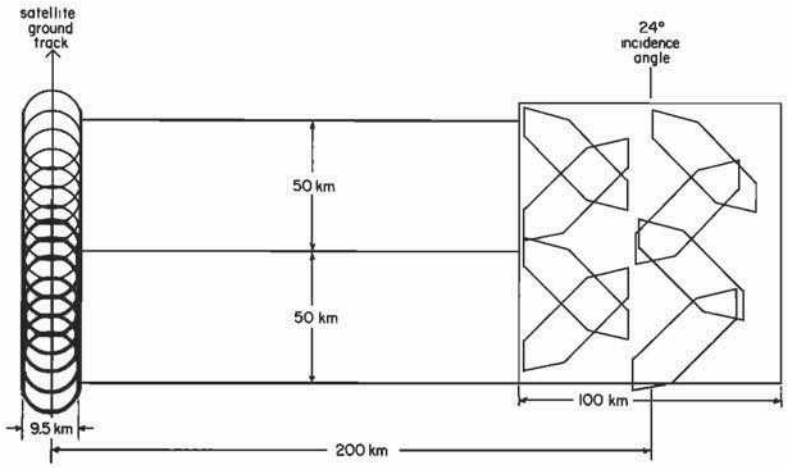

Fig. 1. Approximate geometry of illumination patterns on the sea surface for the Seasat altimeter (ALT) and starboard 24° incidence angle scatterometer (SASS). ALT σ° measurements were averaged into 50 km along-track bins, whereas SASS σ° measurements were averaged into 100 km square cells before computing wind speeds. Thus, each SASS wind cell is associated with two consecutive ALT averages as shown. Heavy and thin lines represent footprints included in two successive 50 km along-track ALT averages.

winds at the sea surface. Thorough discussion can be found in *Moore and Fung* [1979], *Barrick and Swift* [1980] and *Boggs* [1981]. Briefly, the SASS consisted of a pair of 14.6 GHz fan beam antennas on each side of the spacecraft oriented 45° (forward) and 135° (aft) relative to the satellite ground track. The cross-beam width of each antenna was 0.5°. Backscattered radiation was averaged from 61 pulses over a time period of 1.89 s, during which the antenna footprint moves along track a distance of about 12 km on the sea surface. The resulting effective footprint size for the 61 pulse average SASS measurements from a single antenna thus ranged from approximately 16 to 23 km in the cross-beam direction, depending on incidence angle [see *Boggs*, 1981].

The along-beam footprint size for SASS was determined by Doppler filtering the backscattered microwave radiation. Doppler frequency range gates were chosen to break the backscattered signal up into a total of 15 cells with along beam dimension ranging from 50 to 70 km, depending on incidence angle and differing by a small amount for ascending and descending satellite orbits [see *Boggs*, 1981]. Three of these cells were located in the near-nadir regime centered at incidence angles of 0°, 4° and 8°. The remaining 12 cells were located in the off-nadir regime ranging from incidence angles of 22° to 65°.

The physics of radar backscatter is very different for the nadir and off-nadir regimes. In both regimes, backscatter is dependent on wind speed. There is also a wind direction dependence in the off-nadir regime which does not exist at nadir [see *Moore and Fung*, 1979; *Barrick and Swift*, 1980]. Retrieval of both wind speed and direction in the off-nadir regime requires that measurements from the forward and aft antennas be combined in order to separate wind speed effects from wind direction effects on the backscatter. To accomplish this, *Wentz et al.* [1986] binned the SASS measurements into 100 km square cells. For the 24° incidence angle off-nadir cell, the time difference between the forward and aft measurements was about 1 min. Figure 1 shows one such cell on the starboard side of the subtrack. Associated with this 100 km SASS wind cell are two 50 km along-track averaged ALT cells.

There is considerable evidence that accurate estimates of wind speed can be obtained from SASS measurements in the off-nadir regime. This evidence is based on extensive aircraft experiments prior to the launch of Seasat, aircraft underflights during the Seasat mission, and direct comparisons with high quality in situ measurements (see *Boggs* [1981] and *Schroeder et al.* [1982] for summaries of the evolution of the SASS-1 wind speed algorithm). By comparison, evidence for the accuracy of wind speed retrievals from backscatter measurements in the nadir regime is relatively scant. For these reasons, CM proposed using off-nadir SASS measurements of wind speed as "calibration data" to derive a model function for wind speed estimation from ALT measurements of nadir σ°. The temporal and spatial averaging technique used by CM limited the average SASS wind speeds to the range 4–14 ms^{-1}.

We propose a new method of utilizing off-nadir SASS estimates of wind speeds to develop an ALT wind speed model function. The method averages ALT measurements of σ° into 50-km bins in the along-track direction as shown in Figure 1. These averaged ALT measurements are then compared with wind speeds estimated from the nearest off-nadir 100 km binned SASS cells. This technique has been used previously by *Wentz et al.* [1986] to develop a wind speed model function for nadir SASS measurements of σ°. The total number of ALT vs. off-nadir SASS comparisons, using only SASS measurements from the starboard side of the spacecraft, is about 241,000. Port side SASS data were intentionally not used here to develop the ALT wind speed model function in order to retain an independent data set for ALT model function verification. The dynamic range of the individual starboard SASS wind speeds was 0 to 21 ms^{-1}, considerably larger than the 4 to 14 ms^{-1} dynamic range obtained by the temporal and spatial averaging method of CM. The technique proposed here thus yields an ALT wind speed model function which is applicable over a much broader range of wind speeds.

The obvious questionable aspect of this technique is how the 24° incidence angle separation (corresponding to 200 km on the sea surface) between the ALT and SASS data affects the comparison. In addition to random measurement errors, the true wind speed differs at locaions separated by 200 km due to short spatial scale variations in the wind field. How-

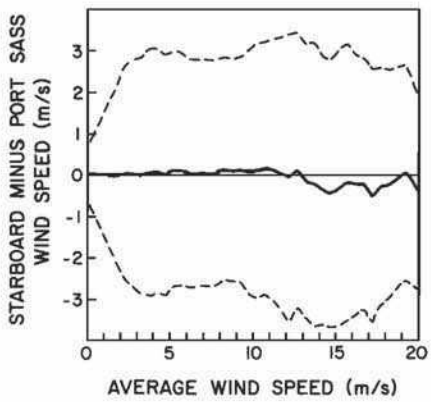

Fig. 2. Comparison of port and starboard SASS measurements at 24° incidence angle computed using the *Wentz et al.* [1986] algorithm. Continuous line represents average difference (starboard minus port) for wind speed bin sizes of 0.5 ms^{-1} and dashed lines correspond to the one standard deviation envelope about the average difference. See text discussion of motivation for using this form of presentation rather than the more common scatter plot of port vs. starboard wind speed.

ever, on average over many comparisons, we expect these true geophysical variations to be random, and thus effectively equivalent to random measurement errors.

To test this hypothesis, we compared starboard and port SASS estimates of wind speed at 24° incidence angles. This corresponds to a spatial separation of approximately 400 km (twice the separation of nadir ALT and nearest off-nadir SASS measurements). Starboard and port SASS wind speed pairs were stratified into 0.5 ms^{-1} bins according to the average of the two wind speeds. The average starboard minus port wind speed for each bin is shown in Figure 2. The dashed lines show the one standard deviation error bars about the averages for each bin. As expected, the figure shows that the average difference between starboard and port wind speeds is very small with typical standard deviations of around 2.7 ms^{-1} within each bin. For wind speed below 13 ms^{-1} the average difference is between -0.17 and 0.15 ms^{-1}. For wind speeds above 13 ms^{-1}, the port wind speed is, on the average, 0.3 ms^{-1} higher than the starboard wind. This small offset is due to the high wind speeds in the southern hemisphere Westerlies (40°S to 65°S). In this region, the Seasat orbit was such that the port cell was always farther south than the starboard cell and thus sampled a higher wind speed on average. Simulations using SASS-derived wind fields show that this latitude wind gradient effect, when averaged globally, produces about a 0.3 m/s bias between the port and starboard 24° incidence angle cells for the high wind speed bins, which agrees with the results shown in Figure 2.

We conclude that both measurement error and geophysical "error" are indeed random over large numbers of measurement pairs, even when separated by 400 km. Note that a standard deviation of 2.7 ms^{-1} corresponds to "errors" of 1.9 ms^{-1} in individual measurements (assuming that the total rms difference of 2.7 ms^{-1} is equally partitioned between port and starboard wind speed errors and that the errors are uncorrelated between port and starboard estimates). As discussed previously, part of this random error represents true differences in the wind speed measurements separated by 400 km.

We point out that the presentation in Figure 2 [previously used by *Wentz et al.* 1986] is preferable to the usual method where port SASS wind speed estimates are plotted against starboard SASS wind speed estimates. The conventional method results in inherent biases at high and low starboard SASS wind speeds. For example, consider a very low wind speed at starboard incidence angle of 24°. Due to mesoscale variations in the wind field, it is likely that the wind speed at port incidence angle of 24° at the same time will be somewhat higher. Similarly, when starboard wind speed is very high, contemporaneous port observations are likely to be somewhat lower. Averaging port and starboard wind speeds, as in the abscissa of Figure 2, eliminates this undesirable bias.

A good ALT wind speed algorithm should show results similar to those shown in Figure 2, i.e., a zero mean difference between ALT and SASS wind speeds when the difference is plotted vs. the average of ALT and SASS wind speeds. We used an iterative procedure to find a relationship between ALT σ° and wind speed that satisfied this criterion. We started by using the CM model function discussed in the Introduction as a first guess for the relation between wind speed and ALT measurements of σ°. As in CM, we used the Hancock algorithm for σ°. The final wind speed model function was then developed in tabular form using the following iterative technique:

1. The first guess CM model function was converted to tabular form for σ° steps of 0.2 dB. Each table entry is the wind speed for the corresponding value of σ°.

2. ALT measurements of σ° were averaged along track over 50 km as discussed previously. The average σ° was then converted to wind speed by linear interpolation from the tabular model function.

3. The resulting ALT estimate of wind speed was compared with the nearest 100 km average starboard SASS estimate of wind speed at 24° incidence angle. The average of the ALT and SASS wind speeds was computed to determine the appropriate average wind speed bin at intervals of 1 ms^{-1}. The ALT minus SASS wind speed difference was then used to accumulate statistics for the corresponding average wind speed bin.

4. Steps 2 and 3 were repeated for all paired ALT and 24° incidence angle starboard SASS wind speeds. Observations with high atmospheric liquid water content, as determined from the Seasat scanning multichannel microwave radiometer, were not included. The resulting total number of paired ALT and SASS observations was 241,000.

5. The overall average ALT minus SASS wind speed was determined for each average wind speed bin. For the first iteration using the CM algorithm in tabular form, many of the bins showed significantly nonzero mean wind speed differences (particularly at high wind speeds). To the extent that the SASS wind speeds are correct, these non-zero mean wind speed differences represent systematic errors in the CM algorithm. To remove these systematic errors, the model function table entries at 0.2 dB steps were adjusted by linear interpolation by half the amount required to give a zero value for the wind speed difference for each average ALT and SASS wind speed bin.

6. Steps 2–5 were then repeated using the new adjusted tabular model function. This iterative procedure was repeated until the binned estimates of ALT minus SASS wind speed converged to zero for each average wind speed bin. The number of iterations required was typically about 5.

3. NEW ALTIMETER WIND SPEED MODEL FUNCTION

The tabular model function derived using the method described in section 2 is given in Table 1. Table values are given in column 2 for σ° (computed by using the Hancock algorithm; see *Chelton and McCabe* [1985]) in steps of 0.2 dB from 8.0 to 19.6 dB. This corresponds to wind speeds ranging from a high of about 21.04 ms^{-1} to a low of about 0.01 ms^{-1}. Tabular values outside of this range were deemed to be unreliable because of the small number of ALT observations less than 8.0 dB and greater than 19.6 dB. This tabular model function is shown by the small dots in Figure 3 in the usual graphical form with wind speed on the abscissa and σ° on the ordinate. The smoothness of this model function relating σ° to wind speed is rather remarkable.

TABLE 1. Raw and Smoothed Tabular Altimeter 19.5 m Wind Speed Model Function Derived by Comparison of Seasat Altimeter σ° With *Wentz et al.* [1986] 24° Incidence Angle Seasat Scatterometer Wind Speed

σ°, dB	Raw $u_{19.5}$, ms^{-1}	Smoothed $u_{19.5}$, ms^{-1}
8.0	21.041	21.080
8.2	20.286	20.341
8.4	19.543	19.571
8.6	18.923	18.767
8.8	18.334	17.920
9.0	17.171	17.019
9.2	16.210	16.069
9.4	14.869	15.079
9.6	14.195	14.062
9.8	13.224	13.026
10.0	11.938	11.982
10.2	10.879	10.939
10.4	9.759	9.907
10.6	8.778	8.892
10.8	7.886	7.909
11.0	7.005	7.007
11.2	6.204	6.222
11.4	5.500	5.531
11.6	4.865	4.910
11.8	4.331	4.360
12.0	3.844	3.877
12.2	3.438	3.452
12.4	3.033	3.088
12.6	2.772	2.787
12.8	2.526	2.527
13.0	2.279	2.286
13.2	2.033	2.073
13.4	1.892	1.902
13.6	1.761	1.761
13.8	1.629	1.629
14.0	1.497	1.497
14.2	1.366	1.366
14.4	1.234	1.236
14.6	1.102	1.120
14.8	1.009	1.031
15.0	0.968	0.971
15.2	0.926	0.926
15.4	0.884	0.884
15.6	0.843	0.843
15.8	0.801	0.801
16.0	0.760	0.760
16.2	0.718	0.718
16.4	0.676	0.676
16.6	0.635	0.635
16.8	0.593	0.593
17.0	0.552	0.552
17.2	0.510	0.510
17.4	0.469	0.469
17.6	0.427	0.427
17.8	0.385	0.385
18.0	0.344	0.344
18.2	0.302	0.302
18.4	0.261	0.261
18.6	0.219	0.219
18.8	0.177	0.177
19.0	0.136	0.136
19.2	0.094	0.094
19.4	0.053	0.053
19.6	0.011	0.011

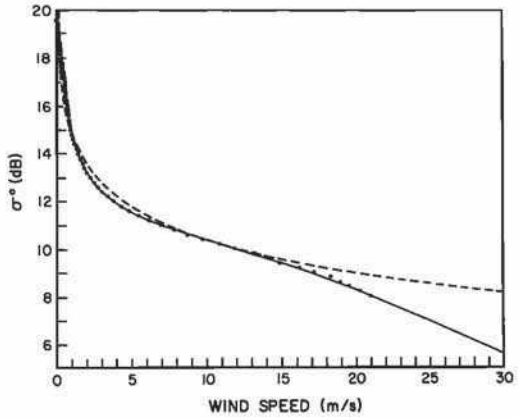

Fig. 3. Graphical presentation of the tabular ALT wind speed model function in Table 1. The dots correspond to the raw values from column 2 of Table 1 and the continuous line corresponds to the smoothed values in column 3 of Table 1. Dashed line represents the power-law ALT model function derived by *Chelton and McCabe* [1985].

It is pointed out in CM that abrupt discontinuities in the slope of any wind speed model function lead to very undesirable results. To assure a smooth model function, the tabular values were smoothed several times with three-point 1-2-1 triangular weighted running average. In addition, although tabular σ° values are limited to the range from 8 to 19.6 dB, values of σ° exceeding 19.6 dB are assumed to correspond to zero wind speed. The high wind speeds (greater than 21 ms^{-1}) corresponding to values of σ° less than 8.0 dB are determined by linear extrapolation from the first two table entries. The resulting final ALT wind speed model function is given in column 3 of Table 1 and shown by the continuous curve in Figure 3.

The performance of this model function is shown in Figure 4. Starboard SASS wind speed at 24° incidence angle and ALT wind speed (determined by linear interpolation from the smoothed table) pairs were stratified into 0.5 ms^{-1} bins according to the average of the two (as in Figure 2). The average ALT minus starboard SASS wind speed for each bin, together with 1 standard deviation error bars, is shown in Figure 4*a*. Recall that only starboard SASS wind speeds were used to derive the ALT wind speed model function. A similar plot comparing port SASS measurements at 24° incidence angle with ALT estimates is shown in Figure 4*b*. For both port and starboard comparisons, the bias in ALT wind speeds is very small (generally less than 0.15 ms^{-1}) over the full range from 0 to 20 ms^{-1}. The standard deviation of ALT minus SASS wind speeds is typically around 2.5 to 3.0 ms^{-1}. The small bias at the high wind speeds for the port comparisons is due to the southern hemisphere latitudinal wind gradient effect discussed in section 2.

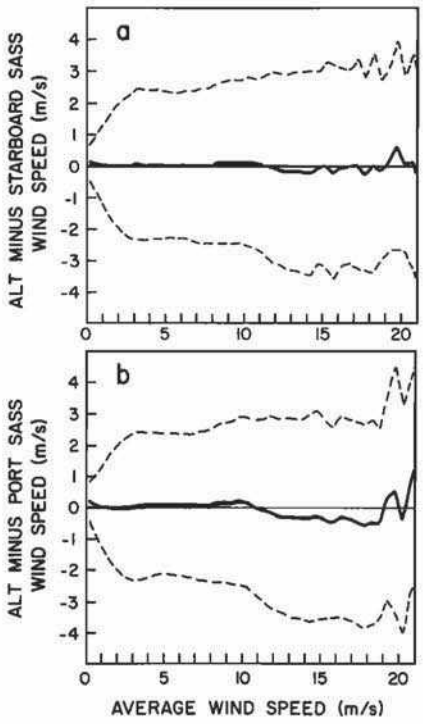

Fig. 4. Comparisons of (*a*) ALT and 24° incidence angle starboard SASS wind speeds; and (*b*) ALT and 24° incidence angle port SASS wind speeds. ALT wind speeds were computed using the smoothed tabular model function in section 3 and SASS wind speeds were computed using the *Wentz et al.* [1986] algorithm. Continuous lines represent the average differences (ALT minus SASS) and dashed lines represent the one standard deviation envelope.

4. Comparison With Previous Wind Speed Model Function

For comparison with the tabular wind speed model function presented in section 3, the power-law model function proposed by CM is shown as the dashed line in Figure 3. It is evident that the two model functions agree very closely for wind speeds up to about 14 ms^{-1}; the CM estimates are slightly low for wind speeds lower than about 1.5 ms^{-1}, and slightly high for wind speeds from about 1.5 to 7 ms^{-1}. At wind speeds greater than 14 ms^{-1}, the two model functions diverge rather dramatically. Since the CM model function was based only on wind speeds in the range 4 to 14 ms^{-1}, it is clearly unreliable at higher wind speeds. The results presented here suggest that at high wind speeds the σ° dependence on wind speed at satellite nadir differs significantly from the simple power-law relation discussed in the Introduction. From Figure 3, a power law relation would overestimate wind speed for small values of σ° (values less than about 9.5 dB). A similar deviation from a constant power law model function was found by *Wentz et al.* [1986] for nadir SASS measurements of σ°.

There are two other comparisons that can be made between ALT wind speeds estimated using the CM model function and the new model function proposed here. Histograms of wind speeds generated from the full Seasat ALT data set are shown by the solid and dashed curves in Figure 5 for the tabular and CM model functions, respectively. The histogram of all off-nadir SASS winds for incidence angles from 24° to 55° is shown by the dotted curve. The SASS histogram is smoother than the ALT histograms because of the much larger number of individual SASS samples over the full range of incidence angles. The new tabular algorithm produces a histogram that is in closer agreement with the SASS histogram than does the CM algorithm.

Finally, the performance of the tabular model function can be tested through a comparison of temporally and spatially averaged ALT and SASS wind speeds, as in CM. A scatter plot of 96-day, 2° latitude by 6° longitude averages is shown in Figure 6*b*. The tabular model function eliminates the suggestion of an overestimate of high wind speeds by ALT obtained using the CM model function (see Figure 6*a*). The tabular model function also eliminates the slight overestimate of wind speeds in the range from 4 to 7 ms^{-1}. These results are consistent with the differences in the two model functions as shown in Figure 3.

We thus conclude that the new tabular ALT wind speed model function proposed here is a considerable improvement over the power-law model function proposed by CM. The tabular model function produces ALT wind speed estimates that are more consistent with SASS wind speeds.

5. Measurements of Nadir σ°

A question of important concern is the general applicability of the ALT wind speed model function presented in section 3. Future satellite altimeter missions will encounter the same difficulties with collection of an adequate high quality in situ data base for calibration of the wind speed algorithm. It is tempting to simply apply wind speed algorithms developed for previous altimeter missions. Indeed, this was the approach followed by the Seasat project to develop a wind speed model function for the Seasat altimeter (see CM for a detailed historical summary). The *Brown et al.* [1981] three-branch wind

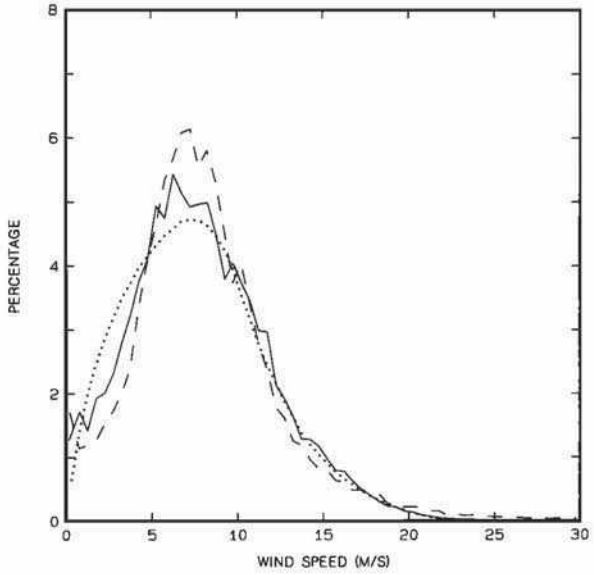

Fig. 5. Histogram of wind speeds for the smoothed tabular ALT model function in Table 1 (continuous curve) and the power-law ALT model function of *Chelton and McCabe* [1985] (dashed curve). The dotted curve shows the histogram for off-nadir SASS winds (all incidence angles) computed using the *Wentz et al.* [1986] algorithm. The winds include the entire Seasat 96-day period for latitude 55°S to 65°N. Bin size is 0.5 ms^{-1}.

speed model function was developed on the basis of comparisons between Geos-3 altimeter measurements of σ° and a total of 184 buoy measurements of wind speed. Seasat ALT measurements of σ° were then calibrated against Geos-3 σ° on the basis of 19 crossovers of the ground tracks of the two satellites. An adjustment was applied to remove a constant relative bias in Seasat σ° and then the Brown et al. Geos-3 wind speed model function was applied directly to the Seasat measurements of σ°.

Seasat provides an opportunity to investigate the validity of applying previously derived wind speed model functions to new satellite measurements of σ°. On Seasat, both ALT and SASS measured σ° at 0° incidence angle. The scattering cross section of the sea surface measured by a satellite radar is defined by the radar equation (see, for example, *Stewart* [1985]),

$$\sigma = \frac{(4\pi)^3 h^4}{t^2 G^2 \lambda^2} \frac{P_R}{P_T}$$

where

- λ the wavelength of the radiation transmitted and received by the radar antenna;
- G the antenna gain;
- h the height of the satellite above the sea surface (800 km for Seasat);
- t the transmittance of the atmosphere (ranging from 1 for a transparent atmosphere to 0 for an opaque atmosphere). For the microwave frequencies of both the Seasat ALT and SASS, t is very nearly 1, except when strong rain cells fall within the antenna footprint;
- P_T the power transmitted by the antenna;
- P_R the return power received by the antenna.

At nadir, σ is determined predominantly by the surface roughness which is related to the wind speed at the sea surface. In addition, the returned power is clearly dependent on the area on the sea surface illuminated by the antenna. This dependence on illumination area can be eliminated by dividing the scattering cross section by the area of the antenna footprint to obtain the normalized radar cross section σ°. For a uniform scattering surface,

$$\sigma^\circ = \frac{\sigma}{A}$$

where A is the area on the sea surface illuminated by the antenna.

The purpose of this rather detailed discussion is to point out that σ° is dependent only on the scattering properties of the sea surface, and not on the area illuminated by the antenna. Thus, although the individual nadir sea surface footprints of the ALT and SASS radars are very different, they should give the same value of σ° if the winds are constant and the same over the ALT and SASS footprints. In the more general case where the winds vary over the ALT and SASS footprints, the two values of σ° may differ. However, in an average sense over many comparisons, the difference between ALT and SASS nadir σ° should be zero.

Recall from section 2 that the gating method used by ALT to measure the return power P_R includes only a portion of the total returned power. The (unnormalized) scattering cross section σ is therefore smaller than the value that would be obtained if the total return of the transmitted power P_T were measured. However, this difference is evidently offset in the calculation of the normalized scattering cross section σ° by use of the gate-limited footprint area rather than the antenna beam-limited footprint area. Thus, ALT measurements of σ° should be equivalent to the values that would be obtained if the total return power were measured and the resulting scattering cross section σ normalized by the beam-limited footprint area.

As discussed previously, each individual ALT measurement at 1 sec intervals (which actually consists of an average over 1020 individual pulses) is approximately a circle with 9.5 km diameter stretched 6.7 km in the along-track direction (a total area of 135 km^2). SASS nadir measurements at 1.89 sec inter-

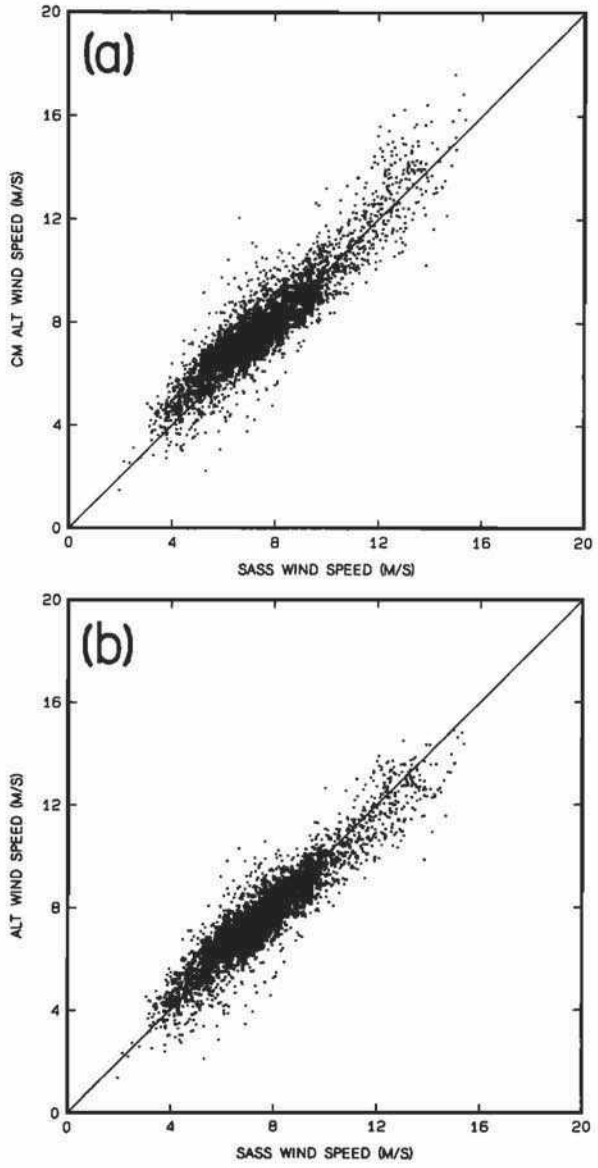

Fig. 6. Scatter plot comparisons of 96-day, nonoverlapping 2° by 6° average ALT wind speeds against SASS wind speeds computed using the *Wentz et al.* [1986] algorithm for the latitude range 55°S to 65°N: (*a*) ALT wind speeds computed using the CM power-law model function; (*b*) ALT wind speeds computed using the smoothed tabular model function in Table 1. Bias and standard deviation, respectively, are (Figure 6*a*) 0.36 ms^{-1} and 0.90 ms^{-1} (Figure 6*b*) 0.04 ms^{-1} and 0.84 ms^{-1}.

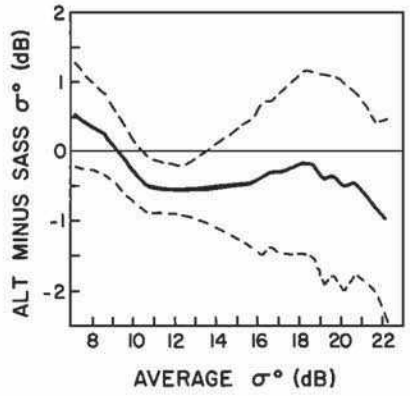

Fig. 7. Comparison of ALT measurements of nadir σ° and SASS measurements of σ° at 0° incidence angle. For both data sets, σ° has been averaged over 50 km in the along-track direction. Continuous line represents average difference (ALT minus SASS) for σ° bin sizes of 0.5 dB and dashed lines correspond to the one standard deviation envelope.

vals (which consist of an average over 61 individual pulses) are approximately a rectangular area with dimensions 16 km by 54 km (an area of 864 km^2) oriented at a 45° angle relative to the satellite subtrack [see *Boggs*, 1981]. To reduce noise inherent in individual measurements, we compared ALT and SASS measurements of nadir σ° averaged over 50 km in the along-track direction. These 50 km averages contain a total of about 7 ALT measurements and 4 SASS measurements (one for each of the four antennas, switched at time intervals of 1.89 s). In these averaged measurements, the total areas illuminated are thus about 945 km^2 and 3456 km^2; the area sampled in these 50 km averages along the satellite subtrack is thus about 4 times larger for SASS than ALT. As noted previously, the two values of 50-km averaged σ° should be the same if the winds were constant over the areas sampled by the two sensors. In general, ALT and SASS measurements of σ° will differ due to mesoscale variability in the wind field but this difference should be zero in an average sense over many comparisons.

In Figure 7, the differences between ALT and SASS 50 km averaged σ° are plotted vs. the average ALT and SASS σ°. These differences represent global averages over 3 months for 0.5 dB σ° bins from 7 to 22.5 dB. It is clear from the figure that there are systematic differences between ALT and SASS measurements of nadir σ°. For σ° less than 9.5 dB, ALT estimates are higher than SASS estimates by as much as 0.5 dB. For σ° greater than 9.5 dB, ALT estimates are low by about 0.5 dB.

While a constant relative bias between ALT and SASS measurements of σ° (such as in the region in Figure 7 where σ° is greater than about 10.5 dB) could easily be explained as a simple calibration error, systematic differences which vary with σ° are very difficult to explain. They must be due either to (1) incorrect prelaunch calibration of either or both the ALT and SASS; or (2) errors in the algorithms used to determine σ° from parameters measured by the instruments (automatic gain control for ALT and voltage for SASS).

We have been unable to identify the source of error for Seasat data. The ALT method of measuring σ° is the most suspect since it uses a gating method to measure only a portion of the total return power. To see how this might affect estimation of σ°, it is necessary to understand the rather complex procedure used to determine σ°. ALT transmits a square pulse of electromagnetic radiation toward the sea surface and measures the return power as a function of time. After the leading edge of the pulse strikes the sea surface, the footprint consists of an expanding circle with area that can be shown to increase linearly with time until the trailing edge of the pulse reaches the sea surface. After this time, the footprint consists of an expanding annulus with constant area. Thus, the returned power increases linearly with time and then becomes constant. (The returned power actually decreases with time in the constant "plateau region" due to the gain on the sides of the main lobe of the antenna.) The leading edge of the linearly increasing return power signal is further stretched due to early returns from wave crests and later returns from wave troughs. Indeed, the slope of the leading edge of the return is used to estimate significant wave height [see *Fedor and Brown*, 1982].

The on-board altitude tracker defines mean sea level to be the point on the stretched leading edge of the return signal where the power is half that of the maximum in the plateau region. This point on the return is then assigned gate 30.5 in a set of 60 gates separated by 3.125 ns with additional gates at 29.5, 30.5 and 31.5. Since the total gate-limited return power is effectively normalized by a fixed area (corresponding to 9.5 km circular footprint) to determine σ° from ALT, any systematic errors in this identification of mean sea level would lead to systematic errors in the computation of σ°. For example, suppose the tracker mistakenly identified mean sea level and that the true mean sea level occurred at gate 29 in the 63 gated samples of the return power. Then the total power computed by the sum over gates 1 through 60 would be about 6.7% higher than if mean sea level were properly assigned to gate 30.5 due to a greater amount of return in the plateau region (2 gates more than would be obtained if the returned power wave form were shifted by 1.5 gates to correctly locate mean sea level at gate 30.5). This could, in principle, be compensated for in the computation of σ° by normalizing by the gate-limited area covered from gate 29 to gate 60 rather than by the fixed area covered from gate 30.5 to gate 60. Note that such systematic tracker errors would also affect sea surface elevation estimates by ALT. *Born et al.* [1982] and *Douglas and Agreen* [1983] have presented evidence that the tracker identification of mean sea level is biased low by an estimated 7% of the siginificant wave height. This bias is due to the combination of an electromagnetic bias caused by a greater return from wave troughs and by the non-Gaussian distribution of wave heights on the sea surface (peaked wave crests and flatter troughs), resulting in a greater fraction of the total returned power backscattered from wave troughs. A correction of 7% was applied to ALT measurements of sea surface elevation to remove these effects. It appears that no such correction was applied to the calculation of σ°.

This error in the tracker identification of mean sea level is small and it is difficult to determine the exact effect it would have on the calculation of σ°. We note, however, that a negative bias in the tracker identification of mean sea level means that true mean sea level occurs in some gate earlier than gate 30.5 as in the example above. Thus, ALT estimates of σ° would be biased due to the presence of waves on the sea surface. Since large waves are generally associated with strong winds (i.e., smaller values of nadir σ°—see Figure 3), this suggests that ALT estimates of σ° would be biased higher for low values of σ°. This is consistent with the results shown in Figure 7, which can be interpreted as an approximately constant relative bias of -0.5 between ALT and SASS for σ°

greater than about 10.5 dB with an approximately linearly increasing bias for smaller values of σ°. If a constant negative bias of -0.5 dB is removed for the full range of σ°, the residual bias would increase approximately linearly with decreasing σ° less than 10.5 dB. The magnitude of this residual bias would range from 0 at a σ° value of 10.5 dB to about 1 dB at a σ° value of 7 dB. A rough calculation assuming a significant wave height of 10 m for a wind speed of 21 m/s (corresponding to σ° value of 8 dB) gives a tracker error of 1.5 gates for a 7% significant wave height correction. This leads to a σ° bias about 40% that of the observed value. This underestimate may be indicative of an error in the tracker bias estimate of 7% of significant wave height.

Clearly, this is an issue that merits further investigation as problems inherent in Seasat data are likely to recur in future satellite missions. For purposes of the presentation here, we conclude that (1) the possibility of an error in the ALT estimation of σ° should be examined in greater detail, and (2) caution must be exercised if the ALT model function presented in section 3 is applied to altimeter measurements of σ° from future satellite missions such as Geosat or TOPEX. Although order 0.5 dB relative biases are small, it can be seen from Figure 3 that they can lead to significant errors in estimates of wind speed, particularly at high wind speeds.

6. Relevance to Geosat

The U.S. Navy recently launched a geodedic satellite Geosat. A Seasat-class altimeter onboard Geosat has operated nearly continuously since March 1985 and has been designed with an expected operational lifetime of at least 3 years. Although sea surface elevation measurements from the Geosat altimeter are classified for the first 18 months of the mission, wind speed estimates will be publicly available from the U.S. Navy. These are the only satellite-measured winds available until at least late 1986 when a passive microwave radiometer will be launched on the next in a series of satellites in the Defense Meteorological Satellite Program. *Niiler* [1985] has proposed using Geosat ALT wind speeds to study ocean-atmosphere latent heat flux (evaporation). It is therefore important to discuss the relevance of the results of this paper to ALT winds from Geosat.

The results of CM were available to the U.S. Navy prior to the launch of Geosat. *Goldhirsh and Dobson* [1985] evaluated the CM model function and the earlier *Brown et al.* [1981] three-branch model function. Arguing that the CM model function was developed without the use of any direct comparisons of ALT σ° with in situ wind observations, Goldhirsh and Dobson recommend a smoothed version of the *Brown et al.* [1981] model function. (Note, however, that the Brown et al. model function was derived from comparisons between in situ measurements of wind speed and the relatively noisy Geos-3 altimeter measurements of σ°.) They smoothed the three-branch model function for wind speed at 10 m above the sea surface by a least squares fit to a fifth order polynomial,

$$\hat{u}_{10}{}^G = a_0 + \sum_{k=1}^{5} a_k(\sigma^\circ)^k$$

The resulting regression parameters are given in Table 2. For comparison with the CM model function and the tabular model function proposed in this paper, these 10 m wind speeds must be converted to a height of 19.5 m. Using a neutral stability wind profile, this results in

$$\hat{u}_{19.5}{}^G = 1.06\ \hat{u}_{10}{}^G$$

This fifth-order polynomial model function is shown in Figure 8. Because of the limited in situ data used to develop the original *Brown et al.* [1981] model function, the *Goldhirsch and Dobson* [1985] smoothed version is applicable only over the range indicated by the heavy continuous curve. The dashed portion of the curve is an extrapolation of the fifth-order polynomial for σ° values less than 7 dB and greater than 15 dB. It is apparent that this model function is incapable of producing wind speeds in excess of 21 ms^{-1}. In addition, the relation between σ° and wind speed in nonunique; the same wind speed can be produced from more than one value of σ°. For small values of σ° (corresponding to high wind speeds), these multiple solutions will not be much of a problem (although the corresponding wind speeds will be significantly underestimated, see Figure 8), since very few ALT measurements of σ° were less than 7 dB. However, a substantial number of ALT measurements of σ° were greater than 15 dB. The performance of the *Goldhirsh and Dobson* [1985] model function at high values of σ° will result in significant overestimates of low wind speed.

It seems clear that the fifth-order polynomial model function recommended by *Goldhirsh and Dobson* [1981] is undesirable as a general model function because of its poor performance outside of the restricted range of σ° values for which it was intended. For comparison, we show the tabular ALT wind speed model function derived in section 3 as the thin continuous curve in Figure 8. Note that the fifth-order polynomial model function considerably underestimates wind speeds greater than 6.5 ms^{-1} and overestimates wind speeds less than 6.5 ms^{-1}.

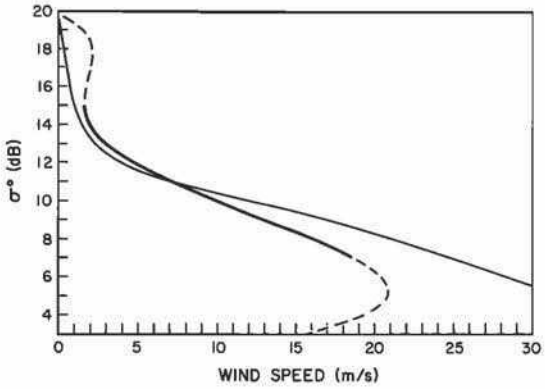

Fig. 8. Comparison of the ALT wind speed model function proposed for the Geosat ALT by *Goldhirsh and Dobson* [1985] (heavy continuous curve and dashed curve) and the smoothed tabular model function in section 3. Heavy continuous portion of the Geosat model function represents the range of values of σ° plotted by *Goldhirsh and Dobson* [1985].

TABLE 2. Coefficients in *Goldhirsh and Dobson* [1985] Fifth-Order Polynomial Fit to *Brown et al.*'s [1981] Three-Branch Altimeter Wind Speed Algorithm

k	a_k
0	-15.383
1	16.077
2	-2.305
3	9.896×10^{-2}
4	1.800×10^{-4}
5	-6.414×10^{-5}

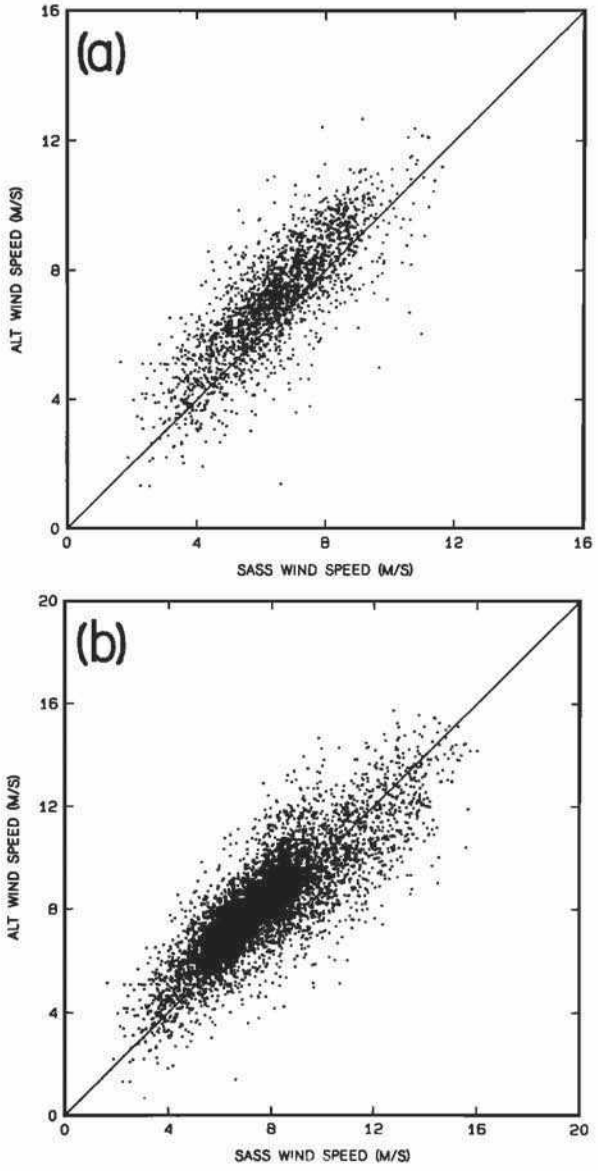

Fig. 9. Similar to Figure 6, except for 2° by 2°, 30-day averages (September 10 through October 9, 1978). (*a*) Scatter plot comparison for the tropical ocean (30°S to 30°N). Bias and standard diviation are 0.66 ms^{-1} and 1.07 ms^{-1}. (*b*) Scatter plot for the global ocean (55°S to 65°N). Bias and standard deviation are 0.38 ms^{-1} and 1.41 ms^{-1}.

Finally, we re-emphasize that caution should be exercised when applying any wind speed model function (including the tabular model function derived in Section 3) developed for a previous satellite altimeter to measurements of σ° from the Geosat altimeter. The results of section 5 suggest that the normalized radar cross section σ° may differ from one radar antenna to another due to calibration and algorithm errors. Note that since the model function for converting σ° to wind speed is inherently nonlinear, a simple constant residual bias in σ° due to calibration errors will not give a constant bias in wind speed.

7. Summary and Conclusions

An earlier altimeter wind speed model function developed by *Chelton and McCabe* [1985] was based on comparisons between 96-day, 2° latitude by 6° longitude averages of ALT measurements of the normalized radar cross section σ° and off-nadir SASS measurements of wind speed. The resulting model function assumed a simple power-law dependence of σ° on wind speed, similar to that suggested previously by *Guinard et al.* [1971] and *Barrick* [1974] and adopted by the Seasat Project for nadir SASS measurements of σ° [*Schroeder et al.*, 1982]. The limitation of this model function derived by Chelton and McCabe is that it was based on comparisons over the restricted range from 4 to 14 ms^{-1}.

In this paper, we have proposed a new model function for ALT estimates of wind speed. This new model function is also based on comparisons between ALT measurements of σ° and SASS off-nadir measurements of wind speed (we used wind speeds produced by the *Wentz et al.* [1986] algorithm). However, rather than temporally and spatially averaging the data as in *Chelton and McCabe* [1985], the comparisons are based on 50 km along-track averages of contemporaneous measurements of ALT σ° at nadir and starboard SASS measurements of wind speed at 24° incidence angle. These measurements are spatially separated by approximately 200 km so that differences in ALT and SASS wind speed are due to both measurement error and short spatial scale variability in the true wind field. Over many comparisons, the average of these two "error" sources is zero.

The resulting model function was developed in tabular form for measurements of σ° from 8.0 to 19.6 dB in steps of 0.2 dB (see Table 1). Measurements of σ° are converted to wind speed by linear interpolation of the table values; values of σ° exceeding 19.6 dB are assigned zero wind speed and wind speeds for values of σ° less than 8.0 dB are determined by linear extrapolation of the first two entries in the table. This tabular model function is valid for wind speeds from 0 to 21.1 ms^{-1}.

A plot of this tabular model function (Figure 3) indicates that the power law relation for σ° assumed by *Chelton and McCabe* [1985] is quite accurate for wind speeds up to 14 ms^{-1}. At higher wind speeds, the tabular model function shows that σ° drops off more quickly than the power-law relation, in agreement with results previously derived for SASS nadir σ° by *Wentz et al.* [1986]. It was shown in section 4 that the tabular model function improves the comparison between temporally and spatially averaged ALT and off-nadir SASS wind speeds.

It is well to keep in mind that, since the ALT wind speed model function developed in this paper was calibrated against SASS wind speeds generated by the *Wentz et al.* [1986] algorithm, the overall accuracy of the resulting ALT winds is only as good as the accuracy of the SASS winds. Thus, if it is determined at some later date that there still remain some systematic errors in the SASS wind speeds, adjustments must be made to the tabular ALT wind speed model function presented in section 3. At present, there is no evidence for any significant systematic errors in the *Wentz et al.* [1986] SASS wind speeds.

In an effort to evaluate the general applicability of the proposed tabular ALT wind speed model function, measurements of nadir σ° from the Seasat ALT and SASS were compared in section 5. It was shown that there are systematic differences between the two measurements of σ°. This is rather surprising since the two measurements should be the same. We have not been able to resolve the discrepancy. It may be due to errors in prelaunch calibration of either or both of the two radars. Alternatively, the discrepancy may be due to errors in the algorithms used to compute σ° from parameters measured by

the two sensors (automatic gain control for ALT and voltage for SASS). ALT is the most suspect because of the complex method used to estimate σ°. On the basis of the results of section 5, caution should be exercised in application of the Seasat ALT wind speed model function to measurements from microwave radars on other satellites. Furthermore, the possibility of an error in the algorithm used to estimate σ° from ALT should be further investigated.

In section 6 we discussed the relevance of the results of this paper to the altimeter on the U.S. Navy satellite Geosat launched in March 1985. Since there are plans to utilize wind speeds from the Geosat altimeter to study ocean-atmosphere latent heat flux [*Niiler*, 1985], careful attention must be given to the model function used to estimate wind speed. It was shown in Section 6 that the model function recommended by *Goldhirsh and Dobson* [1985] has several undesirable properties and should not be adopted as a general model function. We feel that the tabular model function proposed in section 3 is preferable.

One final important question is whether wind fields constructed from ALT data will be sufficiently accurate for studies of ocean-atmosphere latent heat flux (evaporation). The geographical region of primary interest for latent heat flux study is the tropical ocean, from 30°S to 30°N. These studies require a wind speed accuracy of 1.4 ms^{-1} in 2° longitude monthly averages [*Niiler*, 1985]. In section 4, we showed that 2° latitude by 6° longitude averages of ALT wind speeds over the full 96-day Seasat mission agree with average SASS wind speeds to within 0.8 ms^{-1}. Since ALT measured winds over a narrow "swath" width of 9.5 km, compared with a 1500 km swath width for SASS, spatially and temporally averaged wind fields constructed from ALT data are subject to greater errors from sampling variability. These errors increase with decreasing averaging periods and decreasing averaging areas.

A scatter plot of 2° by 2°, monthly average ALT vs. SASS wind speeds (constructed in the same manner as the 96-day averages in Figure 6) is shown in Figure 9. The 30-day period selected here is September 10 to October 9, 1978, which corresponds to the Seasat 3-day repeat orbit period when satellite ground tracks mapped out a grid on the sea surface with approximately 900 km spacing at the equator. This orbit closely resembles that which Geosat will maintain after the first 18 months of the mission. From Figure 9, monthly average wind fields in the tropics constructed from ALT data agree with SASS wind fields to within 1.10 ms^{-1}. A similar comparison of 2° by 2°, monthly averages over the global ocean yields an rms difference of 1.40 ms^{-1}. The increased rms difference when all latitudes are included is, at least in part, due to greater sampling error for the ALT wind speeds due to larger temporal variability of winds outside the tropics. There is a small but significant bias between the ALT and SASS winds for this 30-day period. In the global comparison, ALT winds are about 0.4 ms^{-1} higher than the SASS winds for these 30 days of the Seasat mission. At present, it is not known whether this bias is an artifact of sampling variability or an unexplained temporal change in the relation between σ° and wind speed.

Acknowledgments. This work was carried out at Oregon State University under NASA grant NAGW-730 and at Remote Sensing Systems under NASA contract NASW-4046.

REFERENCES

Barrick, D. E., Wind dependence of quasi-specular microwave sea-scatter, *IEEE Trans. Antennas Propag., AP-22*, 135–136, 1974.

Barrick, D. E., and C. T. Swift, The Seasat microwave instruments in historical perspective, *IEEE J. Oceanic Eng., OE5*, 74–79, 1980.

Boggs, D. H., The Seasat scatterometer model function: The genesis of SASS-1, *Rep. 622-230*, 30 pp., Jet Propul. Lab., Pasadena, Calif., 1981.

Born, G. H., M. A. Richards, and G. W. Rosborough, An empirical determination of the effects of sea state bias on Seasat altimetry, *J. Geophys. Res., 87*, 3221–3226, 1982.

Brown, G. S., H. R. Stanley, and N. A. Roy, The wind speed measurement capability of spaceborne radar altimetry, *IEEE J. Oceanic Eng., OE6*, 59–63, 1981.

Chelton, D. B., and P. J. McCabe, A review of satellite altimeter measurement of sea surface wind speed: With a proposed new algorithm, *J. Geophys. Res., 90*, 4707–4720, 1985.

Douglas, B. C., and R. W. Agreen, The sea state correction for GEOS-3 and Seasat satellite altimeter data, *J. Geophys. Res., 88*, 1655–1661, 1983.

Fedor, L. S., and G. S. Brown, Wave height and wind speed measurements from the Seasat altimeter, *J. Geophys. Res., 87*, 3254–3260, 1982.

Goldhirsh, J., and E. B. Dobson, A recommended algorithm for the determination of ocean surface wind speed using a satellite-borne radar altimeter, *Rep. JHU/APL SIR-85-U005*, Johns Hopkins Univ., Appl. Phys. Lab., Laurel, Md., March 1985.

Guinard, N. W., J. T. Ransone, and J. C. Daley, Variation of the NRCS of the sea with increasing roughness, *J. Geophys. Res., 76*, 1525–1538, 1971.

Jones, W. L., L. C. Schroeder, D. H. Boggs, E. M. Bracalente, R. A. Brown, G. J. Dome, W. J. Pierson, and F. J. Wentz, The Seasat-A satellite scatterometer: The geophysical evaluation of remotely sensed wind vectors over the ocean, *J. Geophys. Res., 87*, 3297–3317, 1982.

Moore, R. K., and A. K. Fung, Radar determination of winds at sea, *Proc. IEEE, 67*, 1504–1521, 1979.

Naval Oceanography Command Detachment, *U.S. Navy Marine Climatic Atlas of the World*, vol. 9, Asheville, N. C., 1981.

Niiler, P. P., Air-sea interaction with SSM/I and altimeter, report, 68 pp., Jet Propul. Lab., Pasadena, Calif., 1985. (Available from Nova Univ./NYIT Press, Fort Lauderdale, Fla.)

Schroeder, L. C., D. H. Boggs, G. Dome, I. M. Halberstam, W. L. Jones, W. J. Pierson, and F. J. Wentz, The relationship between wind vector and normalized radar cross section used to derive Seasat-A satellite scatterometer winds, *J. Geophys. Res., 87*, 3318–3336, 1982.

Stewart, R. H., *Methods of Satellite Oceanography*, 360 pp., University of California Press, Berkeley, Calif., 1985.

Townsend, W. F., An initial assessment of the performance achieved by the Seasat-1 radar altimeter, *IEEE J. Oceanic Eng., OE5*, 80–92, 1980.

Weller, R. A., R. E. Payne, W. G. Large, and W. Zenk, Wind measurements from an array of oceanographic moorings and from F/S *Meteor* during JASIN 1978, *J. Geophys. Res., 88*, 9689–9705, 1983.

Wentz, F. J., S. Peteherych, and L. A. Thomas, A model function for ocean radar cross sections at 14.6 GHz, *J. Geophys. Res., 89*, 3689–3704, 1984.

Wentz, F. J., L. A. Mattox, and S. Peteherych, New algorithms for microwave measurements of ocean winds with application to Seasat and SSM/I, *J. Geophys. Res., 91*, 2289–2307, 1986.

Woiceshyn, P. M., M. G. Wurtele, D. H. Boggs, L. F. McGoldrick, and S. Peteherych, The necessity for a new parameterization of an empirical model for wind/ocean scatterometry, *J. Geophys. Res., 91*, 2273–2288, 1986.

D. B. Chelton, College of Oceanography, Oregon State University, Corvallis, OR 97331.

F. J. Wentz, Remote Sensing Systems, Sausalito, CA 94965.

(Received February 7, 1986;
accepted April 25, 1986.)